THE JOURNAL OF PHYSICAL CHEMISTRY B

Article

pubs.acs.org/JPCB

Multiple Hydrogen-Bonding Interactions of Uric Acid/9-Methyluric Acid with Melamine Identified by Infrared Spectroscopy

Hiroya Asami† and Hiroyuki Saigusa*

Graduate School for Bio- and Nanosystem Sciences, Yokohama City University, 22-2 Seto, Kanazawa-ku, Yokohama 236-0027, Japan

Supporting Information

ABSTRACT: Hydrogen-bonded complexes of uric acid/9-methyluric acid (UA/9MUA) with melamine (MEL) are prepared by the combined technique of laser desorption and supersonic-jet expansion, and their stable structures are investigated by infrared spectroscopy and theoretical calculations. It is shown that the 1:1 complex formed between UA and MEL is of nonplanar type, in which the two chromophore planes are significantly folded and thus allow for triple hydrogen-bonding interactions. An anomalously broad IR band is observed in the low-frequency range 2500−2800 cm^{-1}, which is taken as evidence for the formation of a strong hydrogen bond between one of the NH sites of UA and MEL. In the case of 9MUA, in which hydrogen bonding to the N9H site of UA is blocked by the methyl group, two planar pairs formed of 9MUA and MEL are found to coexist. The nature of the multiple hydrogen-bonding interactions in these complexes is discussed based on the natural bond orbital analysis and compared with those of the guanine−cytosine base pair. The results are expected to provide important information on the structural characterization of urinary stones developed in infants after ingesting MEL-contaminated formula.

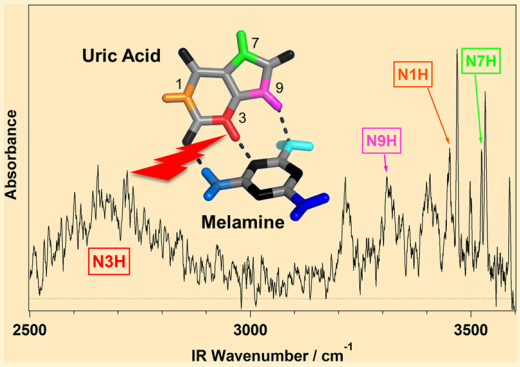

1. INTRODUCTION

Hydrogen bonding (H bonding) has been extensively used for noncovalent synthesis of a variety of supramolecular assemblies including polymers, arrays, and networks. In particular, MEL (Chart 1), a nitrogen-rich organic compound, is known to form

Chart 1. Structures of UA/9MUA and MEL

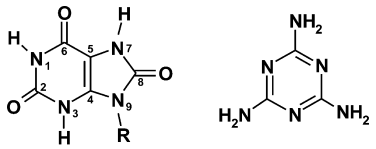

remarkably stable lattices joined by the network of H bonds with cyanuric acid and related compounds.[1−5] MEL is considered to be safe for its normal uses, but food products that are contaminated with it can be unsafe for consumption. It was illegally used for adulterating foods and feeds to mimic the nitrogen content of protein. Later, this contamination was found to cause a series of food safety incidents.[6] Of these incidents, the most serious was the formation of urinary stones in infants ingesting MEL-contaminated formula.[7−9] Analysis of the stones showed that they are composed of MEL and UA (Chart 1) in nearly equimolar amounts[10−12] and suggested that 1:1 H-bonded interaction of the two components may be responsible for the stone formation.[8,13]

Both UA and MEL are nearly insoluble in cold water, but it was found that repeated sonication and shaking of a 1:1 mixture in water results in the formation of an elastic hydrogel.[14] A possible structure of the gel, which is likely to be an assembly of H-bonded complexes formed of UA and MEL, was explored by the powder X-ray diffraction method combined with structural calculations. The result suggested that the hydrogel is composed of two distinct H-bonding rearrangements of the complementary donor (D)−acceptor (A) pair.

In this work, binary complexes consisting of UA/9MUA and MEL are produced in the gas phase by laser desorption, and their structural characterization is performed by the technique of IR−UV double-resonance spectroscopy.[15] Several structural isomers are possible for UA/9MUA owing to keto−enol tautomerization that may take place between adjacent CO and NH sites. Our previous results indicated that only triketo form of UA/9MUA shown in Chart 1 is present in the UV spectra, with no evidence of enol form.[16] Monohydrated clusters of UA were also studied to gain microscopic information on its hydrophobic property. Two prominent monohydrate structures were identified as those with UA in the triketo form.[16]

Here we show that the 1:1 complex of UA and MEL possesses a nonplanar structure with the UA plane slightly folded with respect to MEL and stabilized by multiple H-bonding interactions. In the case of 9MUA, in which nonplanar

Received: March 17, 2014
Revised: April 11, 2014
Published: April 14, 2014

   dx.doi.org/10.1021/jp502635w | J. Phys. Chem. B 2014, 118, 4851−4857

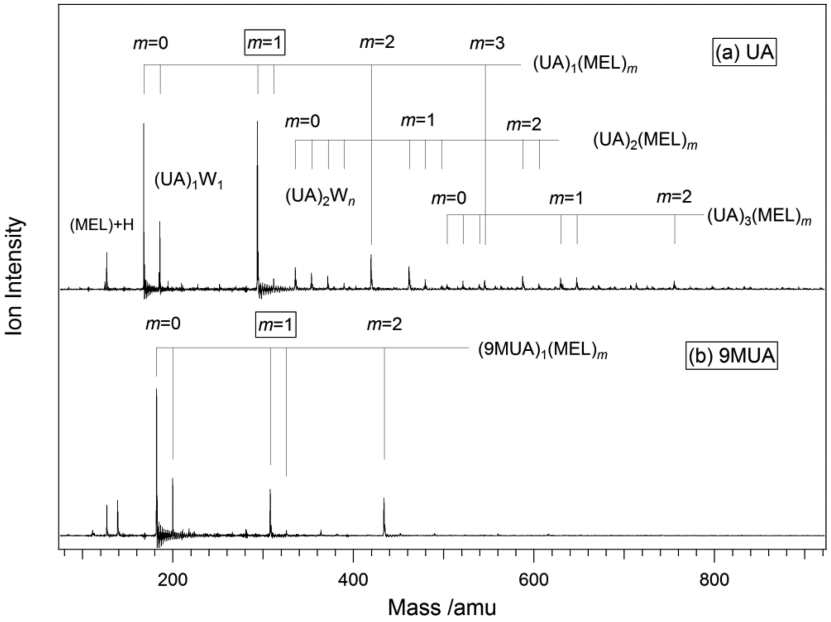

Figure 1. Typical TOF mass spectra showing 1:1 complexes (indicated by $m = 1$) of (a) UA−MEL and (b) 9MUA−MEL. Hydrated clusters with sizes of water molecules n are indicated by W_n.

structures are energetically unstable, two structural isomers of planar type are observed in the UV spectrum. The nature of these H-bonding interactions is discussed based on the natural bond orbital (NBO) analysis[17,18] and compared with the Watson−Crick base pair formed between guanine and cytosine (G−C).

2. EXPERIMENTAL AND CONPUTATIONAL METHODS

The compounds of UA and 9MUA tend to decompose upon heating and thus vaporized by the laser desorption technique, as described in detail elsewhere.[19,20] A sample pellet was prepared by mixing the samples of UA/9MUA and MEL (1:1 in molar ratio) with a graphite matrix (10%) and irradiated by the 532 nm output of a YAG laser (Continuum Surelite). The plume of desorbed molecules was entrained into a supersonic expansion of argon (5 atm) to facilitate complex formation.

Various complexes formed by this method were ionized through resonant two-photon ionization (R2PI) using a frequency-tunable UV laser and analyzed by a TOF mass spectrometer. Mass-selected electronic spectra were recorded by probing ion signal at a particular mass channel while scanning UV laser frequency. IR spectra were recorded in the region 2500−3700 cm^{-1} by an IR−UV double-resonance scheme[21,22] but not normalized with respect to the IR laser power (5−10 mJ/pulse). The UV light was the frequency-doubled output of a YAG-pumped dye laser (Continuum Surelite/ND6000) operated at 10 Hz, while the IR light was generated at 5 Hz using an OPO/OPA system (LaserVision) pumped by a YAG laser (Continuum Powerlite8000). The alternate UV signals measured with IR laser turned on and off were fed into a boxcar integrator and converted into the absorbance scale.

Geometries of the UA/9MUA−MEL complexes were optimized at the MP2 level of theory with the 6-311++G(d,p) basis set. Thereafter, single-point calculations were carried out for the lower-energy structures at the CCSD level with the same basis set to improve the accuracy of their energetic ordering. For complex geometries with relative energies of <14 kJ/mol, vibrational frequency calculations were performed at the B3LYP/6-311++G(d,p) level.

To evaluate H-bond strengths of the UA/9MUA−MEL complex, NBO analyses were employed. In the NBO model,[17,18] H-bonding interaction associated with an H bond A−H···B is considered as electron delocalization from a lone-pair orbital of B to an antibonding σ^*(A−H) orbital. The delocalization energy is evaluated by the second-order perturbation energy $E_{i\rightarrow j}$, in which i and j indicate the ith lone pair orbital of B and the jth antibonding orbital, respectively. The calculation was performed at the B3LYP/6-311++G(d,p) level.

3. RESULTS AND DISCUSSION

3.1. TOF and UV Spectra. The time-of-flight (TOF) mass spectra recorded for mixtures of UA/9MUA and MEL are shown in Figure 1. In the case of UA shown in Figure 1a, mass peaks associated with complexes consisting of UA and MEL are indicated by $(UA)_l(MEL)_m$. The most prominent peak observed at $m/z = 294$ is assigned to the 1:1 complex $(UA)_1(MEL)_1$, hereafter denoted as UA−MEL. Also noted is the appearance of mass peaks corresponding to hydrated clusters of UA, as marked by $(UA)_lW_n$ ($l = 1,2$) even though no water vapor was added in the expansion. In contrast, clusters containing both MEL and water molecules $(UA)_1(MEL)_mW_n$ are found to be scarce, which suggests that complexation of UA with MEL is likely to accommodate few water molecules. This tendency is more evident in the TOF spectrum obtained with trace amounts of water. (See Figure S1 in Supporting Information) Figure 1b presents the mass spectrum obtained for a mixture of 9MUA and MEL, which reveals a mass peak at $m/z = 308$ corresponding to the $(9MUA)_1(MEL)_1$ complex denoted by 9MUA−MEL.

Figure 2 compares the UV spectra recorded by scanning the UV laser frequency while probing the ion signal of UA/9MUA−MEL. Both of the complex spectra appear to be broad with no reproducible peaks, although the respective monomer spectra consist of sharp and underlying broad features. The

dx.doi.org/10.1021/jp502635w | J. Phys. Chem. B 2014, 118, 4851−4857

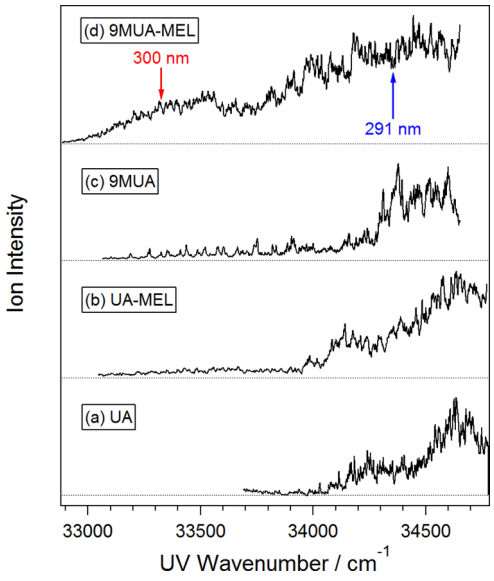

Figure 2. UV spectra of (a) UA, (b) UA–MEL, (c) 9MUA, and (d) 9MUA–MEL. The arrows indicated in panel d correspond to the UV frequencies (in nanometers), which are used to record the IR spectra of the 9MUA–MEL complex.

complex spectra are not significantly displaced from those of the respective monomers, an indication that the electronic excitation in these complexes is localized on the UA/9MUA chromophore and MEL is acting as a solvent.

3.2. UA–MEL Complex. The IR spectrum recorded for the UA–MEL complex in the region 2500–3600 cm^{-1} is displayed in Figure 3b. The IR spectral pattern was nearly independent of the probe UV frequency range of >34 000 cm^{-1} (Figure 2b), which indicates that a single structural isomer accounts for the UV spectrum in this frequency range. Attempts to record IR spectra in the UV frequency region of <34 000 cm^{-1} have failed because of its low R2PI signal. In the observed IR spectrum, it is evident that the two bands appearing at 3449 and 3524 cm^{-1} correspond well to the stretching transitions of N1H (shown in orange) and N7H (green) of the triketo form of UA shown in Figure 3a.[16] The other two free NH stretching transitions of UA, namely, N3H (red) and N9H (pink), are absent in the IR spectrum, and thus possible complex geometries are associated with those with these NH sites H bonded to MEL. It is also important to note that a significantly broadened transition appears in the frequency range 2500–2800 cm^{-1}, which suggests the formation of strong H bonding between the two chromophores. Other sharp and broad peaks indicated by the respective frequencies in black are due to stretching vibrations of the H-bonded NH sites and those of the NH_2 stretches of MEL.

Low-energy structures of the UA–MEL complex calculated at the MP2 level of theory with the 6-311++G(d,p) basis set are shown in Figure 4. The two most stable structures correspond to nonplanar pairs formed by triple H bonding between UA and MEL. In the global minimum denoted as structure 239 (top left), the O2 atom of UA acts as a proton acceptor (A), while the N3H and N9H sites act as double donors (D), thus allowing for ADD(UA)–DAA(MEL) type. This structure is calculated to be more stable by 3.0 kJ/mol than structure 893 (top right). The preferential stabilization of the nonplanar structures by H bonding can be rationalized by a theoretical prediction that the N3/N9 protons are more acidic than the N1/N7 protons,[23] which is also consistent with the result obtained for monohydrated clusters.[16]

In contrast, planar or nearly planar pairs appear to be higher in energy as a result of the significant pyramidarization of the amino groups of MEL, which is in agreement in part with a previous theoretical prediction.[14] The most stable planar structures are of ADA–DAD type, as denoted by 678 and 216, which are unstable by >5 kJ/mol than the global minimum structure 239. For each planar structure, two slightly different geometries are calculated to be stable: In one (denoted by the suffix "-1"), two molecular planes are tilted along the middle H

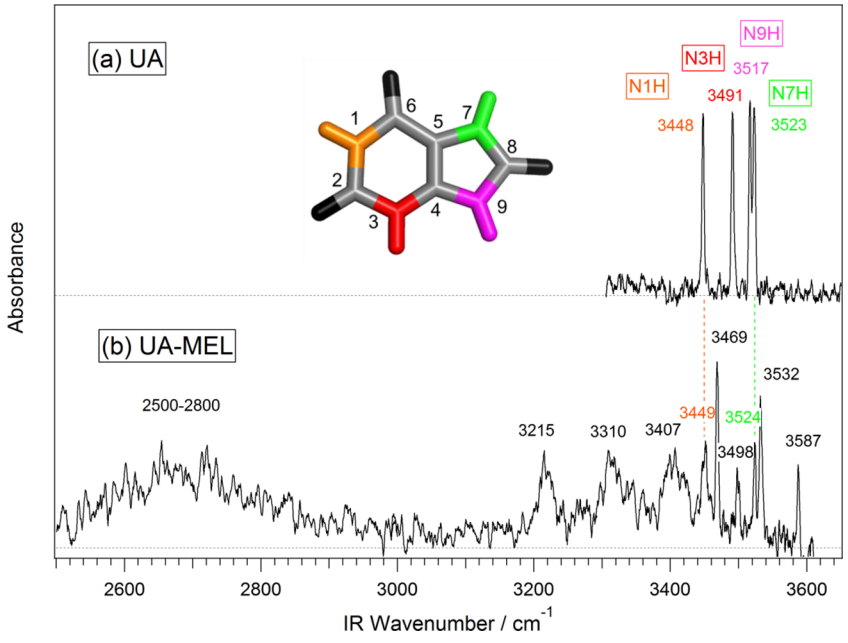

Figure 3. Experimental IR spectra of (a) UA monomer and (b) UA–MEL complex. Vibrational assignments of the respective NH stretch sites of UA are indicated in color.

dx.doi.org/10.1021/jp502635w | J. Phys. Chem. B 2014, 118, 4851–4857

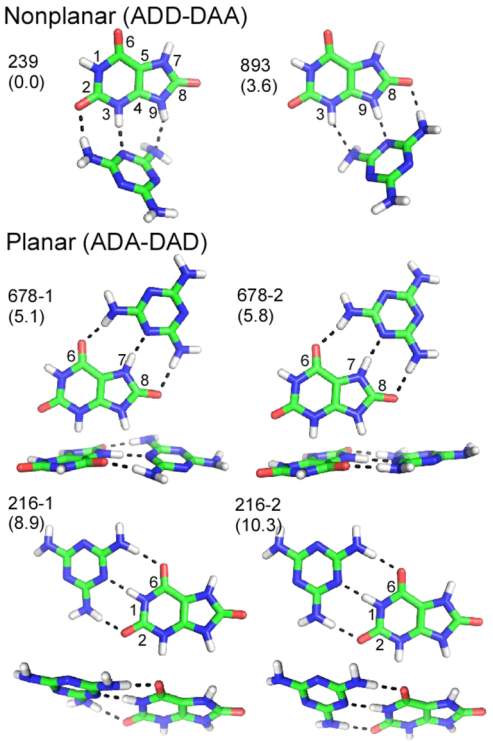

Figure 4. Low-energy structures calculated for the UA−MEL complex. Stabilization energy (in kilojoules per mole) with respect to the most stable structure denoted as 239 is shown in parentheses. The three digit number indicates the relevant UA sites (either ADD or ADA type), which are H bonded to MEL. Two slightly different conformers are calculated to be stable for each planar structure and are indicated by "-1" and "-2".

bond, while in the other (denoted by "-2"), they are almost coplanar. Subsequent single-point energy calculation showed that these two structures are close in energy, as indicated. Stacked structures (no shown) are found to be significantly high in energy by >14 kJ/mol.

In previous clinical analyses of urinary stones detected in infants ingesting MEL-contaminated formula, it was speculated that such planar H-bonding interactions of ADA−DAD type shown in Figure 4 are involved in the stone formation.[8,13] Likewise, structural analysis of the hydrogel formed of UA and MEL by the powder X-ray diffraction method showed that these two planar structures account for about two-thirds of the low-energy crystal structures.[14]

The IR spectrum of the UA−MEL complex shown in Figure 3 clearly indicates that neither N1H nor N7H site of UA is occupied by H bonding, ruling out the possibility of the planar structures of 678 and 216. Thus, the observed UA−MEL complex is assigned to either structure 239 or 893. The calculated vibrational frequencies for these nonplanar structures are shown in Figure 5.

To distinguish between the two possible nonplanar structures, we consider the vibrational frequencies associated with the NH_2 stretches of MEL. The sharp peak observed at 3498 cm^{-1} is assigned to the antisymmetric stretching vibration of the NH_2 group that is H bonded to the NH site of UA, either N9H of structure 239 or N3H of structure 893. This peak is located nearly in the middle of the two transitions due to the N7H stretch (3524 cm^{-1}) and the symmetric stretch of the free NH_2 group [sNH_2(free), 3469 cm^{-1}]. Thus, it is

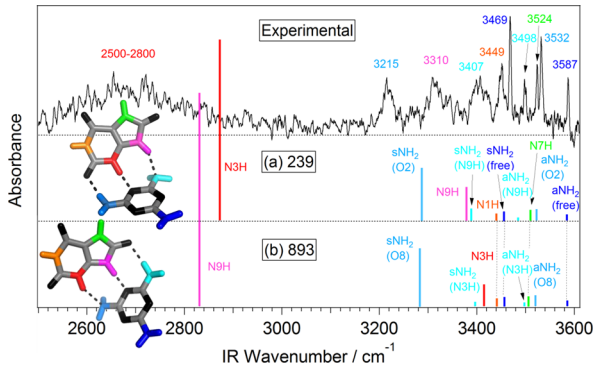

Figure 5. Vibrational frequencies (scaled by a factor of 0.955) and IR intensities calculated for nonplanar structures (a) 239 and (b) 893 shown in inset. Vibrational assignments and corresponding stretch sites of UA and MEL are indicated in color. Experimental IR spectrum (top) is reproduced from Figure 3b.

consistent more with the spectral pattern calculated for structure 239 shown in Figure 5a. In structure 893, the corresponding transition, indicated as aNH_2(N3H), is calculated to be in close proximity to the N7H stretch transition. This prediction is also supported by the result of an NBO analysis, as described later.

The vibrational frequency calculation also predicts that the vibrational frequency of the NH stretch in UA that is associated with the middle H bond, for example, N3H and N9H in structures 239 and 893, respectively, shifts well below 3000 cm^{-1}. As previously explained, transitions associated with the free N3H and N9H stretches of UA are absent in the IR spectrum, which suggests that the observed broad IR transition corresponds to either of the two NH stretching vibrations. On these bases, the UA−MEL complex is assigned to that of the most stable structure 239. This observation is consistent with our previous results for monohydrates of UA, in which the two most stable forms of similar stabilization energies were detected, presumably due to effective cooling pertinent to our desorption method.[16] Calculated vibrational frequencies for the two most stable planar structures 678 and 216 shown in Figure 4 are summarized in Supporting Information (Figure S2).

3.3. 9MUA−MEL Complex. Because methylation of UA at its N9H site prevents the formation of nonplanar pairs of 239 and 893, it is expected that the most stable structures of the 9MUA−MEL complex are of planar type. As shown in Figure 6, the relative energies calculated for structures 678 and 216 are essentially similar to those of the UA−MEL complex shown in Figure 4. Furthermore, there exist two nearly isoenergetic structures with slightly different geometries, as in the case of the UA−MEL complex. We have also carried out geometry optimization at the B3LYP level with the 6-311++G(d,p) basis set and found that only one conformer is stable for each of structures 678 and 216. Since the vibrational frequencies of these planar structures are calculated at the same level of theory, the result is shown for this conformer.

The results of IR−UV double-resonance measurements on the 9MUA−MEL complex are shown in Figure 7. They were obtained with the UV laser fixed at 300 and 291 nm for R2PI as indicated in the UV spectrum in Figure 2d. It is obvious that spectral pattern differs for the two probe frequencies. In the spectrum of Figure 7a recorded with the UV laser fixed at 300 nm, a peak corresponding to the N1H stretch of 9MUA monomer appears at 3449 cm^{-1} in Figure 7c, while peak

dx.doi.org/10.1021/jp502635w | J. Phys. Chem. B 2014, 118, 4851−4857

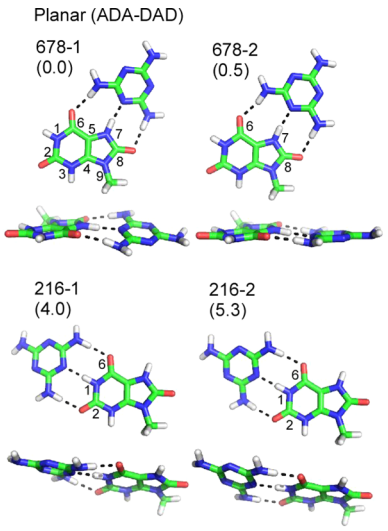

Figure 6. Low-energy structures calculated for the 9MUA−MEL complex. The three digit number indicates the three UA sites (ADA), which are H bonded to MEL. Two slightly different conformers obtained for the planar structures are indicated by "-1" and "-2". Stabilization energy (in kilojoules per mole) with respect to the most stable structure denoted as 678-1 is shown in parentheses.

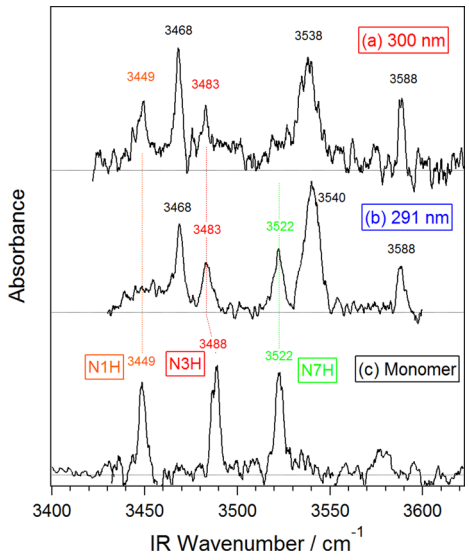

Figure 7. IR spectra of 9MUA−MEL complex recorded with UV laser fixed at (a) 300 and (b) 291 nm, which are indicated by arrows in Figure 2d. (c) IR spectrum of 9MUA monomer.

assignable to the N7H stretch is absent from the spectrum. This firmly establishes that the observed complex corresponds to structure 678 shown in Figure 6. It should also be emphasized that this spectral pattern is nearly independent of the UV frequency in the range <34 000 cm^{-1}. In contrast, the IR spectrum in Figure 7b (obtained at 291 nm) reveals a pronounced peak due to the N7H stretch at 3522 cm^{-1}, with no noticeable peak corresponding to the monomer N1H stretch. Thus, it is assigned to structure 216, in which neither N3H nor N7H site is involved in H bonding. In both cases, a peak assignable to the free N3H stretching vibration is observed at 3483 cm^{-1}, somewhat red-shifted from that of the monomer at 3488 cm^{-1}. This spectral shift is explained by the occurrence of structural deformation of the N3 atom with respect to the six-membered ring upon complexation with MEL, in agreement with the result of vibrational frequency calculations (Figure S3 in Supporting Information).

The IR spectrum of the planar structure 678 extended in the low-frequency range is depicted in Figure 8a. Analogous to the

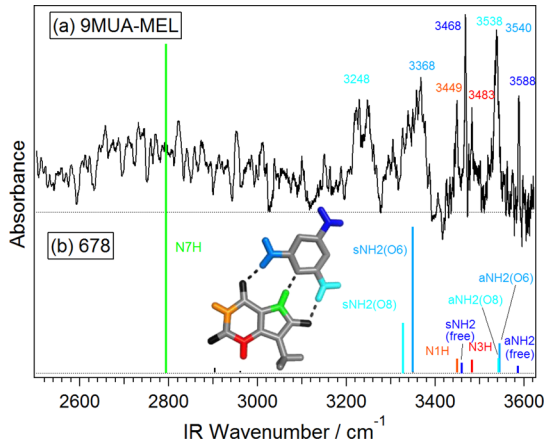

Figure 8. (a) Extended IR spectrum of 9MUA−MEL complex probed at 300 nm. (b) Vibrational frequencies (scaled by a factor of 0.955) and IR intensities calculated for the planar structure 678 shown in inset. Vibrational assignments and corresponding stretch sites of UA and MEL are indicated in color.

nonplanar structure 239 of the UA−MEL complex, broad features appear in the frequency range centered at ~2800 cm^{-1}. This transition is unambiguously assigned to the donor N7H stretch, as predicted by the calculated IR spectrum shown in Figure 8b. Similar broad, red-shifted IR transitions are observed in IR spectrum of structure 216, as shown in Figure 9a. In this structure, MEL is strongly H-bonded to the N1H site, and thus the corresponding vibrational transition results in a substantial red shift.

Finally, we would like to discuss why the less stable structure 216 is predominantly detected by the R2PI method, as opposed to the result for the UA−MEL complex. Furthermore, the UV spectrum of 678 structure (~300 nm, as indicated in Figure 2d) is considerably red-shifted with respect to that of structure 216 (~291 nm). To account for this apparently anomalous

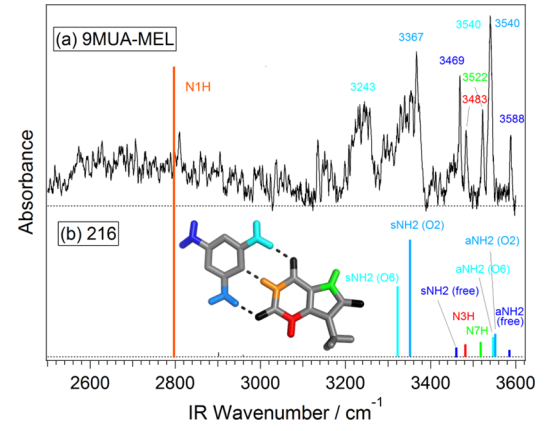

Figure 9. (a) Extended IR spectrum of 9MUA−MEL complex probed at 291 nm. (b) Vibrational frequencies (scaled by a factor of 0.955) and IR intensities calculated for the planar structure 216 shown in inset. Vibrational assignments and corresponding stretch sites of UA and MEL are indicated in color.

dx.doi.org/10.1021/jp502635w | J. Phys. Chem. B 2014, 118, 4851−4857

observation, their minimum-energy structures and excitation energies in the lowest $\pi\pi^*$ state have been calculated by the TDDFT (time-dependent density functional theory) method with a 6-311G(d,p) basis set. A preliminary result, which shown in Table S1 of Supporting Information, reveals that the vertical excitation energy of structure 678 is lower by ∼0.1 eV than in structure 216. Although the calculated excitation energies appear to be somewhat larger than the experimental values, the energy difference is in qualitative agreement with the observed one. The lowering of the excitation energy is likely to occur as a result of ring deformation in 9MUA as well as structural rearrangement of MEL in its excited state (Figure S4 in Supporting Information), which are apparently less pronounced in structure 216. In addition, the oscillator strength calculated for structure 216 is larger than that for structure 678 (Table S1 in Supporting Information). In relation to this observation, a recent theoretical result showed that the lowest $\pi\pi^*$ excitation energy calculated for a specific monohydrate structure of UA, in which water is hydrated to the N7H and O6 sites, is lower by 0.2 to 0.3 eV than that for other monohydrated structures.[24] This behavior was attributed to the stabilization of the π^* orbital induced by H bonding with the O6 site.

3.4. NBO Analyses. It is evident from the above results that the formation of triple H bond is responsible for the large stabilization of the UA/9MUA−MEL complexes, apparently analogous to that of the Watson−Crick G−C base pair. To elucidate the nature of these multiple H-bonding structures in more detail, we have employed the NBO analysis, which is used to evaluate the delocalization energy associated with H bonding.[17,18] The results obtained for the two most stable structures in the each complex are summarized in Figure 10. In

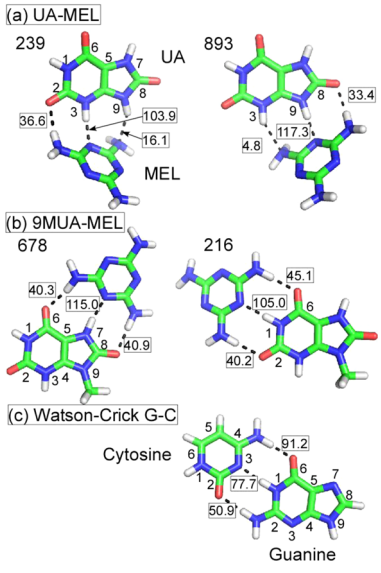

Figure 10. Delocalization energies calculated for H-bonding interactions (shown in boxes in kilojoules per mole): (a) structures 239 and 893 of UA−MEL complex; (b) structures 678 and 216 of 9MUA−MEL complex; (c) G−C base pair.

the case of structure 239 of UA−MEL shown in Figure 10a (left), the delocalization energy estimated for the H bond of N3−H···N is 103.9 kJ/mol, while the corresponding energies for the other H bonds O2···H−N and N9−H···N are much lower (36.6 and 16.1 kJ/mol, respectively). Thus, the stability of this complex is largely associated with the formation of the middle H bond. In striking contrast, the delocalization energies estimated for the G−C base pair (Figure 10c) are nearly comparable for the three H bonds, ranging between 50 and 92 kJ/mol. This difference in the delocalization energy of H bonding is manifested in their IR spectra. The IR spectrum obtained for the G−C base pair reveals that the three stretching vibrations involved in the triple H bonding, namely, N1H and sNH_2 of G and sNH_2 of C, are observed in the region of 3000−3200 cm^{-1}.[25] In the UA−MEL complex, the vibrational frequency of the N3H stretch that is involved in the middle H bonding is further red-shifted down to ∼2600 cm^{-1}, while the other NH stretch (N9H) is less shifted (∼3310 cm^{-1}), as shown in Figure 5. In addition, the delocalization energy of the H bond N9−H···N (16.1 kJ/mol) is calculated to be substantially larger than that of the corresponding H bond N3−H···N in structure 893 (4.8 kJ/mol), which reinforces the assignment that the observed IR peak at 3498 cm^{-1} shown in Figure 3b is that of structure 239.

The results of NBO analysis for the 9MUA−MEL complex are shown in Figure 10b. In both structures 678 and 216, the delocalization energy associated with the middle H bond appears to be dominant, and the other two H bonds give rise to lower delocalization energies of 40−45 kJ/mol. This result is different from the case of the nonplanar structures, in which the delocalization energies of the three H bonds are substantially different, as previously described. It is therefore suggested that formation of triple H bonding is geometrically less restricted in the planar structures than in the nonplanar structures.

4. CONCLUSIONS

Structural characterization of the 1:1 complexes formed between UA/9MUA and MEL has been performed by IR spectroscopic measurements combined with theoretical calculations. It is found that the UA−MEL complex possesses a nonplanar structure, which corresponds to the calculated most stable structure, as stabilized by multiple H-bonding interactions. A significantly red-shifted, broad IR transition is observed in the range 2500−2800 cm^{-1} and assigned to the stretching vibration of the NH bond that is strongly H bonded to MEL. This spectroscopic evidence combined with additional NBO analyses shows that the interaction of UA with MEL is quite local, with one of the three H bonds being extremely robust.

Two distinct structural isomers have been observed for the 9MUA−MEL complex and identified as the calculated most stable structures of planar type. Such planar structures were suggested to be responsible for the formation of urinary stones and hydrogels, both found to be composed of complementary UA and MEL pairs. This specific H-bond interaction is in contrast with that of the G−C base pair, in which the delocalization energies of the three H bonds are nearly comparable.

Structural characterization of UA−MEL complexes and their hydrates of larger sizes is expected to provide important information for a possible cause of urinary stone formation previously observed in infants who ingested melamine contaminated formula.

■ ASSOCIATED CONTENT

Supporting Information

TOF mass spectra recorded for a mixture of UA and MEL in the presence of water vapor, IR frequencies calculated for the low-energy structures of the UA−MEL and 9MUA−MEL

dx.doi.org/10.1021/jp502635w | J. Phys. Chem. B 2014, 118, 4851−4857

complexes, and lowest $\pi\pi^*$ excitation energies of the 9MUA−MEL complex.

This material is available free of charge via the Internet at http://pubs.acs.org.

AUTHOR INFORMATION

Corresponding Author

*E-mail: saigusa@yokohama-cu.ac.jp. Phone: +81-45-787-2179.

Present Address

[†]H.A.: Department of Life Science, Graduate School of Bioscience and Biotechnology, Tokyo Institute of Technology, Yokohama 226-8501, Japan

Notes

The authors declare no competing financial interest.

ACKNOWLEDGMENTS

This work was supported by the Grant-in-Aid from JSPS (25410023) and by the Grant-in-Aid for Scientific Research in the priority area "Molecular Science for Supra Functional Systems" from MEXT. H.A. acknowledges graduate fellowship support from JSPS (22008000, 25002918). We also thank Shuhei Urashima for experimental assistance.

REFERENCES

(1) Whitesides, G. M.; Simanek, E. E.; Mathias, J. P.; Seto, C. T.; Chin, D. N.; Mammen, M.; Gordon, D. M. Noncovalent Synthesis: Using Physical-Organic Chemistry to Make Aggregates. *Acc. Chem. Res.* **1995**, *28*, 37−44.

(2) Ranganathan, A.; Pedireddi, V. R.; Rao, C. N. R. Hydrothermal Synthesis of Organic Channel Structures: 1:1 Hydrogen-Bonded Adducts of Melamine with Cyanuric and Trithiocyanuric Acids. *J. Am. Chem. Soc.* **1999**, *121*, 1752−1753.

(3) Perdigão, L. M. A.; Champness, N. R.; Beton, P. H. Surface Self-Assembly of the Cyanuric acid−Melamine Hydrogen Bonded Network. *Chem. Commun.* **2006**, 538−540.

(4) Zhang, X.; Chen, T.; Chen, Q.; Wang, L.; Wan, L. J. Self-Assembly and Aggregation of Melamine and Melamine−Uric/Cyanuric Acid Investigated by STM and AFM on Solid Surfaces. *Phys. Chem. Chem. Phys.* **2009**, *11*, 7708−7712.

(5) Ciesielski, A.; Haar, S.; Paragi, G.; Kupihár, Z.; Kele, Z.; Masiero, S.; Guerra, C. F.; Bickelhaupt, F. M.; Spada, G. P.; Kovács, L.; Samorì, P. Supramolecular H-bonded Porous Networks at Surfaces: Exploiting Primary and Secondary Interactions in a Bi-Component Melamine−Xanthine System. *Phys. Chem. Chem. Phys.* **2013**, *15*, 12442−12446.

(6) Ingelfinger, J. R. Melamine and the Global Implications of Food Contamination. *N. Engl. J. Med.* **2008**, *359*, 2745−2748.

(7) Sharma, K.; Paradakar, M. The Melamine Adulteration Scandal. *Food Secur.* **2010**, *2*, 97−107.

(8) Skinner, C. G.; Thomas, J. D.; Osterloh, J. D. Melamine Toxicity. *J. Med. Toxicol.* **2010**, *6*, 50−55.

(9) Reimschuessel, R.; Puschner, B. Melamine Toxicity — Stones vs. Crystals. *J. Med. Toxicol.* **2010**, *6*, 468−469.

(10) Lam, C.; Lan, L.; Che, X.; Tam, S.; Wong, S.; Chen, Y.; Jin, J.; Tao, S. H.; Tang, X.; Yuen, K.; et al. Diagnosis and Spectrum of Melamine-Related Renal Disease: Plausible Mechanism of Stone Formation in Humans. *Clin. Chim. Acta* **2009**, *402*, 150−155.

(11) Guan, N.; Fan, Q.; Ding, J.; Zhao, Y.; Lu, J.; Ai, Y.; Xu, G.; Zhu, S.; Yao, C.; Jiang, L.; et al. Melamine-Contaminated Powdered Formula and Urolithiasis in Young Children. *N. Engl. J. Med.* **2009**, *360*, 1067−1074.

(12) Grases, F.; Costa-Bauzá, A.; Gomila, I.; Serra-Trespalle, S.; Alonso-Sainz, F.; del Valle, J. M. Melamine Urinary Bladder Stone. *Urology* **2009**, *73*, 1262−1263.

(13) Cong, X.; Sun, X.; Ning, B. Could Infrared Spectroscopy Identify Melamine-Related Stone Using Melamine-Contained Mixture as a Reference? *J. Clin. Lab. Anal.* **2013**, *27*, 59−61.

(14) Anderson, K. M.; Day, G. M.; Paterson, N. J.; Byrne, P.; Clarke, N.; Steed, J. W. Structure Calculation of an Elastic Hydrogel from Sonication of Rigid Small Molecule Components. *Angew. Chem., Int. Ed.* **2008**, *47*, 1058−1062.

(15) Zwier, T. S. Laser Spectroscopy of Jet-Cooled Biomolecules and Their Water-Containing Clusters: Water Bridges and Molecular Conformation. *J. Phys. Chem. A* **2001**, *105*, 8827−8839.

(16) Asami, H.; Urashima, S.; Saigusa, H. Structural Identification of Uric Acid and Its Monohydrates by IR−UV Double Resonance Spectroscopy. *Phys. Chem. Chem. Phys.* **2011**, *13*, 20476−20480.

(17) Reed, A. E.; Curtiss, L. A.; Weinhold, F. Intermolecular Interactions from a Natural Bond Orbital, Donor-Acceptor Viewpoint. *Chem. Rev.* **1988**, *88*, 899−926.

(18) Sakota, K.; Kageura, Y.; Sekiya, H. Cooperativity of Hydrogen-Bonded Networks in 7-Azaindole $(CH_3OH)_n$ (n = 2,3) Clusters Evidenced by IR-UV Ion-Dip Spectroscopy and Natural Bond Orbital Analysis. *J. Chem. Phys.* **2008**, *129*, 054303−054310.

(19) Saigusa, H.; Tomioka, A.; Katayama, T.; Iwase, E. A Matrix-Free Laser Desorption Method for Production of Nucleobase Clusters and Their Hydrates. *Chem. Phys. Lett.* **2006**, *418*, 119−125.

(20) Saigusa, H. Excited-State Dynamics of Isolated Nucleic Acid Bases and Their Clusters. *J. Photochem. Photobiol., C* **2006**, *7*, 197−210.

(21) Asami, H.; Urashima, S.; Tsukamoto, M.; Motoda, A.; Hayakawa, Y.; Saigusa, H. Controlling Glycosyl Bond Conformation of Guanine Nucleosides: Stabilization of the Anti Conformer in 5′-*O*-Ethylguanosine. *J. Phys. Chem. Lett.* **2012**, *3*, 571−575.

(22) Asami, H.; Yagi, K.; Ohba, M.; Urashima, S.; Saigusa, H. Stacked Base-Pair Structures of Adenine Nucleosides Stabilized by the Formation of Hydrogen-Bonding Network Involving the Two Sugar Groups. *Chem. Phys.* **2013**, *419*, 84−89.

(23) Chandra, A. K.; Zeegers-Huyskens, Th. Theoretical Study of the Acidity and Basicity of Uric Acid and its Interaction with Water. *J. Mol. Struct. (THEOCHEM)* **2007**, *811*, 215−221.

(24) Yamazaki, S.; Urashima, S.; Saigusa, H.; Taketsugu, T. Ab Initio Studies on the Photophysics of Uric Acid and its Monohydrates: Role of the Water Molecule. *J. Phys. Chem. A* **2014**, *118*, 1132−1141.

(25) Abo-Riziq, A.; Grace, L.; Nir, E.; Kabelác, M.; Hobza, P.; de Vries, M. S. Photochemical Selectivity in Guanine−Cytosine Base-Pair Structures. *Proc. Natl. Acad. Sci. U.S.A.* **2005**, *102*, 20−23.